

The centrality dependence of transverse energy and charged particle multiplicity at RHIC: Statistical model analysis

Dariusz Prorok*

Institute of Theoretical Physics, University of Wrocław,

Pl. Maksa Borna 9, 50-204 Wrocław, Poland

(Dated: December 23, 2004)

The transverse energy and charged particle multiplicity at midrapidity are evaluated in a statistical model with the longitudinal and transverse flows for different centrality bins at RHIC at $\sqrt{s_{NN}} = 130$ and 200 GeV. Full description of decays of hadron resonances is applied in estimations of the ratio. The predictions of the model at the freeze-out parameters, established independently from observed particle yields and p_T spectra, agree qualitatively well with the experimental data. The observed overestimation of the ratio can be explained for more central collisions by redefinition of $dN_{ch}/d\eta|_{mid}$.

PACS numbers: 25.75.-q, 25.75.Dw, 24.10.Pa, 24.10.Jv

I. INTRODUCTION

In the previous paper [1] the extensive analysis of two measured global variables, transverse energy ($dE_T/d\eta|_{mid}$) and charged particle multiplicity ($dN_{ch}/d\eta|_{mid}$) densities at mid-rapidity, was delivered. The analysis was done in the framework of the single freeze-out statistical model [2, 3, 4] for the most central collision cases of AGS, SPS and RHIC. Now the same method will be applied in the examination of the centrality dependence of the above-mentioned variables and their ratio. The main idea of this method is as follows. Thermal and geometric parameters of the model are established from fits to particle yield ratios and p_T spectra, respectively. Then, with the use of these parameters both densities, $dE_T/d\eta$ and $dN_{ch}/d\eta$, can be estimated numerically and compared with the data. The first part of this two-step prescription has been already done for the existing mid-rapidity data for different centrality bins at RHIC at $\sqrt{s_{NN}} = 130$ and 200 GeV [5, 6]. In the present paper the second step will be performed, namely the estimations of $dE_T/d\eta|_{mid}$ and $dN_{ch}/d\eta|_{mid}$ for these centralities and comparison with the data reported in Refs. [7, 8, 9, 10]. The main reason for doing it is that the transverse energy and charged particle multiplicity measurements are independent of hadron spectroscopy (in particular, no particle identification is necessary), therefore they could be used as an additional test of the self-consistency of a statistical model. There is also an additional pragmatic reason: predictions of variety of theoretical models were confronted with the data in [10], but none of these models was a statistical model.

The experimentally measured transverse energy is defined as

$$E_T = \sum_{i=1}^L \hat{E}_i \cdot \sin \theta_i , \quad (1)$$

where θ_i is the polar angle, \hat{E}_i denotes $E_i - m_N$ (m_N means the nucleon mass) for baryons, $E_i + m_N$ for antibaryons and the total energy E_i for all other particles, and the sum is taken over all L emitted particles [10].

As a statistical model the single freeze-out model is taken (for details see [5]). The model succeeded in the accurate description of ratios and p_T spectra of particles measured at RHIC [2, 3, 4]. The main postulate of the model is the simultaneous occurrence of chemical and thermal freeze-outs, which means that the possible elastic interactions after the chemical freeze-out are neglected. The conditions for the freeze-out are expressed by values of two independent thermal parameters: T and μ_B . The strangeness chemical potential μ_S is determined from the requirement that the overall strangeness equals zero.

The second basic feature of the model is the complete treatment of resonance decays. This means that the final distribution of a given particle consists not only of the thermal part but also of contributions from all possible decays and cascades.

*Electronic address: prorok@ift.uni.wroc.pl

II. THE FOUNDATIONS OF THE SINGLE-FREEZE-OUT MODEL

The main assumptions of the model are as follows: (a) the chemical and thermal freeze-outs take place simultaneously, (b) all confirmed resonances up to a mass of 2 GeV from the Particle Data Tables [11] are taken into account, (c) a freeze-out hypersurface is defined by the equation

$$\tau = \sqrt{t^2 - r_x^2 - r_y^2 - r_z^2} = \text{const} , \quad (2)$$

(d) the four-velocity of an element of the freeze-out hypersurface is proportional to its coordinate

$$u^\mu = \frac{x^\mu}{\tau} = \frac{t}{\tau} \left(1, \frac{r_x}{t}, \frac{r_y}{t}, \frac{r_z}{t} \right) , \quad (3)$$

(e) the transverse size is restricted by the condition $r = \sqrt{r_x^2 + r_y^2} < \rho_{\max}$. This means that two new parameters of the model have been introduced, *i.e.* τ and ρ_{\max} , which are connected with the geometry of the freeze-out hypersurface.

The invariant distribution of the measured particles of species i has the form [3, 4]

$$\frac{dN_i}{d^2 p_T dy} = \int p^\mu d\sigma_\mu f_i(p \cdot u) , \quad (4)$$

where $d\sigma_\mu$ is the normal vector on a freeze-out hypersurface, $p \cdot u = p^\mu u_\mu$, u_μ is the four-velocity of a fluid element and f_i is the final momentum distribution of the particle in question. The final distribution means here that f_i is the sum of primordial and simple and sequential decay contributions to the particle distribution (for details see [1, 5]).

The pseudorapidity density of particle species i is given by

$$\frac{dN_i}{d\eta} = \int d^2 p_T \frac{dy}{d\eta} \frac{dN_i}{d^2 p_T dy} = \int d^2 p_T \frac{p}{E_i} \frac{dN_i}{d^2 p_T dy} . \quad (5)$$

Analogously, the transverse energy pseudorapidity density for the same species can be written as

$$\frac{dE_{T,i}}{d\eta} = \int d^2 p_T \hat{E}_i \cdot \frac{p_T}{p} \frac{dy}{d\eta} \frac{dN_i}{d^2 p_T dy} = \int d^2 p_T p_T \frac{\hat{E}_i}{E_i} \frac{dN_i}{d^2 p_T dy} . \quad (6)$$

For the quantities at midrapidity one has (in the c.m.s., what is the RHIC case)

$$\frac{dN_i}{d\eta} \Big|_{mid} = \int d^2 p_T \frac{p_T}{m_T} \frac{dN_i}{d^2 p_T dy} , \quad (7)$$

$$\frac{dE_{T,i}}{d\eta} \Big|_{mid} = \begin{cases} \int d^2 p_T p_T \frac{m_T - m_N}{m_T} \frac{dN_i}{d^2 p_T dy} , & i = \text{baryon} \\ \int d^2 p_T p_T \frac{m_T + m_N}{m_T} \frac{dN_i}{d^2 p_T dy} , & i = \text{antibaryon} \\ \int d^2 p_T p_T \frac{dN_i}{d^2 p_T dy} , & i = \text{others} . \end{cases} \quad (8)$$

Note that for the older data from RHIC at $\sqrt{s_{NN}} = 130$ GeV [8] the *antibaryon* case is not distinguished and the corresponding expression for the transverse energy density is the same as for all other particles.

The overall charged particle and transverse energy densities can be expressed as

$$\frac{dN_{ch}}{d\eta} \Big|_{mid} = \sum_{i \in B} \frac{dN_i}{d\eta} \Big|_{mid} , \quad (9)$$

$$\frac{dE_T}{d\eta} \Big|_{mid} = \sum_{i \in A} \frac{dE_{T,i}}{d\eta} \Big|_{mid} , \quad (10)$$

where A and B ($B \subset A$) denote sets of species of finally detected particles, namely the set of charged particles $B = \{\pi^+, \pi^-, K^+, K^-, p, \bar{p}\}$, whereas A also includes photons, K_L^0 , n and \bar{n} [8].

TABLE I: Values of thermal and geometric parameters of the model for various centrality bins taken from [5, 6]. Marked are these bins, for which values of geometric parameters have been obtained by the author from linear approximation between the nearest neighbours (see the text for the explanation).

Collision case	Centrality [%]	N_{part}	τ [fm]	ρ_{max} [fm]
PHENIX at $\sqrt{s_{NN}} = 130$ GeV: $T = 165$ MeV, $\mu_B = 41$ MeV	0-5	348	8.20	6.90
	5-15*	271	7.49	6.30
	15-30	180	6.30	5.30
	30-60*	79	4.62	3.91
	60-92	14	2.30	2.0
PHENIX at $\sqrt{s_{NN}} = 200$ GeV: $T = 165.6$ MeV, $\mu_B = 28.5$ MeV	0-5	351.4	7.86	7.15
	5-10*	299.0	7.48	6.81
	10-15*	253.9	7.10	6.47
	15-20*	215.3	6.71	6.13
	20-30	166.6	6.14	5.62
	30-40	114.2	5.73	4.95
	40-50	74.4	4.75	3.96
	50-60	45.5	3.91	3.12
	60-70	25.7	3.67	2.67
	70-80	13.4	3.09	2.02
STAR at $\sqrt{s_{NN}} = 200$ GeV: $T = 165.6$ MeV, $\mu_B = 28.5$ MeV	0-5	352	9.74	7.74
	5-10	299	8.69	7.18
	10-20	234	8.12	6.44
	20-30	166	7.24	5.57
	30-40	115	7.07	4.63
	40-50	76	6.38	3.91
	50-60	47	6.19	3.25
	60-70*	27	5.70	2.51
	70-80	14	5.21	1.76

III. RESULTS

Analyses of the particle ratios and p_T spectra at various centralities in the framework of the single freeze-out model were done for RHIC in [5, 6]. The results of fits are gathered in table I. Since not all bins reported in [12, 13, 14] were fitted, the lacking values of the geometric parameters have been obtained from the linear approximation between the nearest up and down neighbours. This is justify because the geometric parameters, when plotted as a function of centrality, show roughly linear dependence [6]. Also in table I the corresponding number of participants (N_{part}) is given for each bin. If the division into centrality classes is different for the identified charged hadron measurements and the $dE_T/d\eta$ and $dN_{ch}/d\eta$ measurements, values of N_{part} are taken from reports on the former. Therefore N_{part} values from [12, 15] are listed for PHENIX, whereas N_{part} values for STAR are taken from its transverse energy measurement analysis [9] (in [13, 14] values of N_{part} are not given).

The results of numerical estimations of $dN_{ch}/d\eta|_{mid}$ divided by the number of participant pairs for PHENIX centrality bins tabulated in table I are presented in figs. 1 and 2 for $\sqrt{s_{NN}} = 130$ and 200 GeV respectively. Additionally to the straightforward PHENIX measurements of the total charged particle multiplicity, also the data from the summing up of the integrated charged hadron yields are depicted in these figures (more precisely, since the integrated charged hadron yields are given as rapidity densities, the transformation to pseudo-rapidity should be done, which means the division by a factor 1.2 here, see [16]). This is because fits of the parameters of the model should be done to the same p_T spectra which are to be integrated to delivered the charged hadron yields. For PHENIX at $\sqrt{s_{NN}} = 200$ GeV this is not true since fits were done to the preliminary data [13], but the integrated charged hadron yields were delivered in the final report [15]. And as one can see from a comparison between figures in [13] and [15], points from the former are slightly above corresponding points from the latter. To estimate the scale of this difference, the sum of integrated charged hadron yields at $N_{part} = 114.2$ (the point of the biggest discrepancy between the model evaluation and the experimental data, see fig. 2) has been obtained again from digitizing the data depicted in preliminary plots in [13].

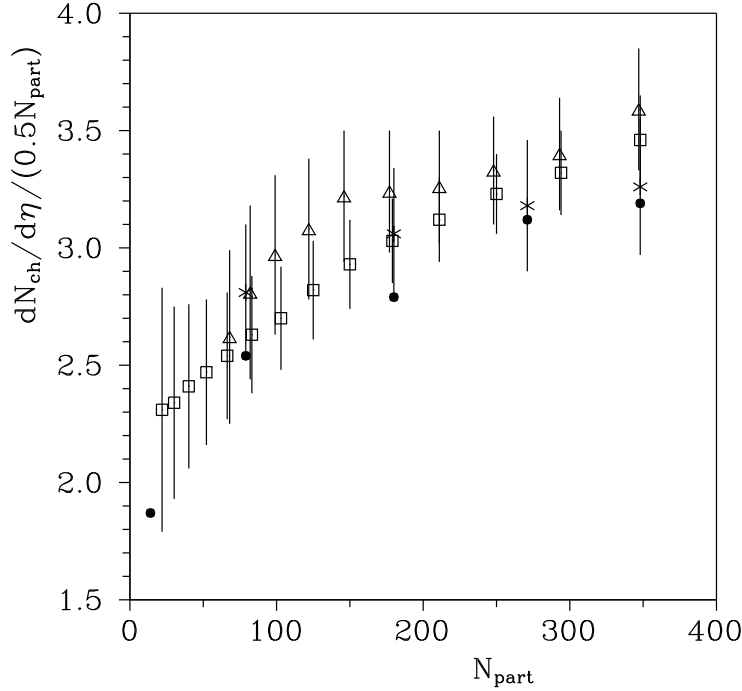


FIG. 1: $dN_{ch}/d\eta$ per pair of participants versus N_{part} for RHIC at $\sqrt{s_{NN}} = 130$ GeV. Dots denote model evaluations, squares the newest PHENIX data [10], triangles the earlier reported PHENIX data [7] and crosses are the recalculated PHENIX data from summing up the integrated charged hadron yields delivered in [12].

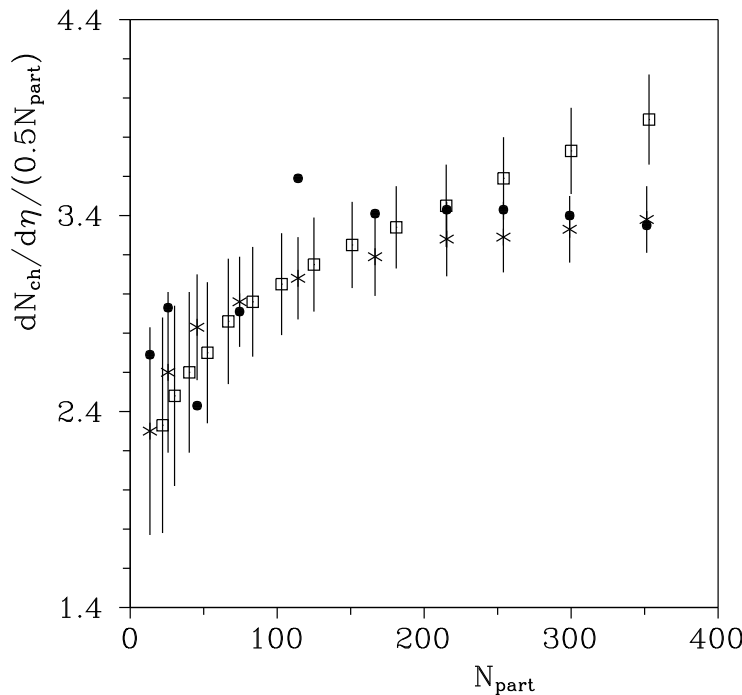


FIG. 2: $dN_{ch}/d\eta$ per pair of participants versus N_{part} for RHIC at $\sqrt{s_{NN}} = 200$ GeV. Dots denote model evaluations, squares PHENIX data [10] and crosses are the recalculated PHENIX data from summing up the integrated charged hadron yields delivered in [15].

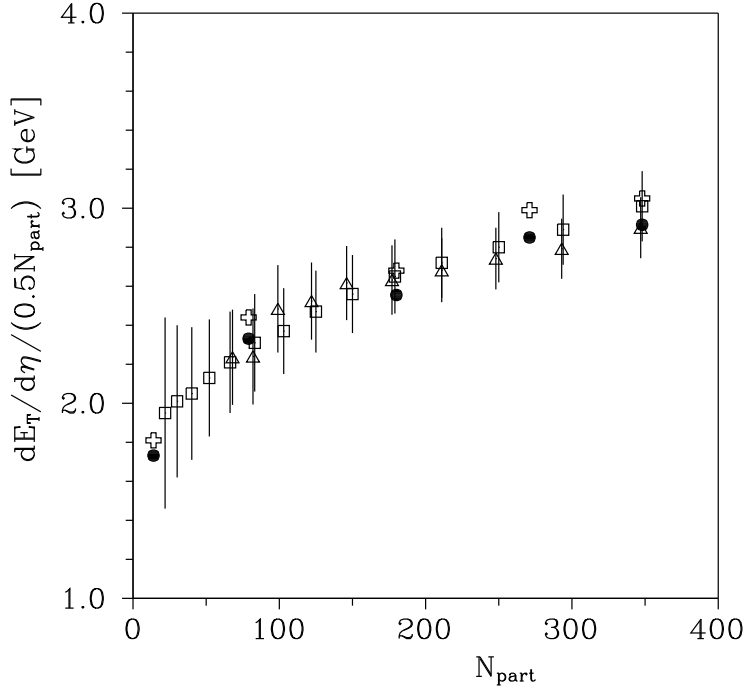


FIG. 3: $dE_T/d\eta$ per pair of participants versus N_{part} for RHIC at $\sqrt{s_{NN}} = 130$ GeV. Dots and open crosses denote model evaluations, triangles and squares are PHENIX data [7, 10]. Dots and triangles are for the older definition of E_T , *i.e.* the total energy E_i is taken also for antibaryons in eq. (1).

This gives 3.31 of charged particles per participant pair, which is exactly 10% above the value obtained from the data given in [15]. And the model evaluation is only 8.5% greater than this number. Also in [15] the feeding of $p(\bar{p})$ from $\Lambda(\bar{\Lambda})$ decays is excluded, contrary to [13]. Therefore, the model estimates should overestimate the corresponding recalculated experimental values for PHENIX at $\sqrt{s_{NN}} = 200$ GeV. To diminish this effect, integrated p and \bar{p} yields delivered in [15], were corrected to include back the feeding. The correction was done by the division by a factor 0.65, which is rough average of a p_T dependent multiplier used by PHENIX Collaboration (see fig.4 and eq.(5) in [15]). Since all just stated reasons for the "systematic" discrepancies affect the absolute values of $dN_{ch}/d\eta|_{mid}$, they reveal themselves in the normalization factor τ^3 in the model (see eq. (10) in [1]). For PHENIX at $\sqrt{s_{NN}} = 130$ GeV the same spectra were used to fit the model parameters and to obtain the integrated yields [12], so the predictions should agree with the recalculated data in principle. As one can notice from figs. 1 and 2, the above comments concerning both PHENIX measurements are true. The greatest overestimation is in the most peripheral bin and in the mid centrality region of the measurements at $\sqrt{s_{NN}} = 200$ GeV. But even at the worst point the model prediction is 17% over the corresponding recalculated experimental value. It is not so bad because the absolute value of theoretical $dN_{ch}/d\eta$ is determined by the factor τ^3 . This means that the 5.3% uncertainty in τ is enough to cause the 17% uncertainty in $dN_{ch}/d\eta$. The second reason for the quantitative disagreement is that transverse momentum spectra are measured in *limited ranges*, so very important low- p_T regions are not covered by the data. To obtain integrated yields some extrapolations below and above the measured ranges are used. In fact these extrapolations are only analytical fits, but contributions from regions covered by them account for about 25 – 40% of the integrated yields [12]. It might turned out that these extrapolations differ from the thermal distributions supplemented by the distributions of products of decays.

Generally, the agreement of the model predictions with the data is much better for RHIC at $\sqrt{s_{NN}} = 130$ GeV. For the case of $\sqrt{s_{NN}} = 200$ GeV, only the rough qualitative agreement has been reached and the reasons have just been explained. It is also worth to stress once more, that the discrepancy between the directly measured $dN_{ch}/d\eta$ and $dN_{ch}/d\eta$ expressed as the sum of the integrated charged hadron yields can be one of these reasons, especially for RHIC at $\sqrt{s_{NN}} = 200$ GeV (see fig 2; this effect has already been notified in backup slides of [13]). The discrepancy starts at mid-centrality and rises with the centrality.

The values of $dE_T/d\eta|_{mid}$ divided by the number of participant pairs are shown in figs. 3 and 4 for $\sqrt{s_{NN}} = 130$ and 200 GeV respectively. The quality of the model predictions for $dE_T/d\eta$ is the same as for $dN_{ch}/d\eta$ in the PHENIX case. Again, the worst agreement is for the case of $\sqrt{s_{NN}} = 200$ GeV but the overestimation is higher and equals

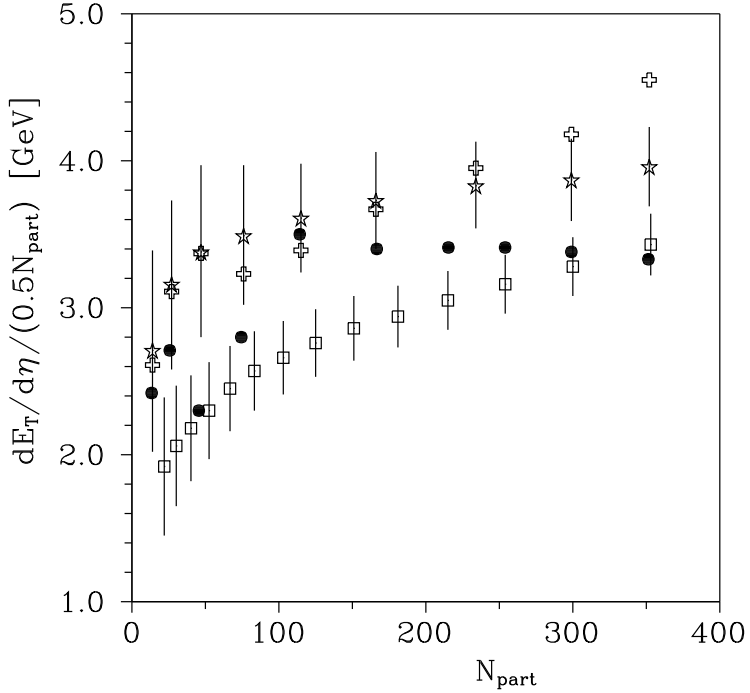


FIG. 4: $dE_T/d\eta$ per pair of participants versus N_{part} for RHIC at $\sqrt{s_{NN}} = 200$ GeV. Dots and open crosses denote model evaluations, squares and stars are data. Dots and squares are for PHENIX (data from [10]), open crosses and stars for STAR (original data from [9] have been rescaled to $\eta = 0$, see the text for the explanation).

30% at most. The main source of the overestimation seems to be the same as in the $dN_{ch}/d\eta$ case, namely the uncertainty of fitting the parameter τ . The STAR measurements need separate comments. The STAR data were taken not at mid-rapidity ($\eta = 0$) as in the PHENIX case but at $\eta = 0.5$ [9]. But the p_T spectra used for fits of the geometric parameters were measured at mid-rapidity, also in the STAR case [14]. Therefore one should expect some "systematic" discrepancy between predictions and the data on the whole. To remove this effect the original STAR data [9] have been divided by a factor $\sin(\theta|_{\eta=0.5}) \approx 0.887$. As it can be seen from fig. 4, the predictions and data agree with each other within errors besides the most central point. But even there, the discrepancy does not overcome 15%. Of course, the second source of the disagreement could be the uncertainty in τ (in fact, as it will be seen, it seems to be the main source of the disagreement in all discussed cases). It should be also noticed that bigger values of transverse energy estimates for the STAR case are the consequence of higher values of p_T distributions of pions, kaons and antiprotons measured by STAR Collaboration with respect to PHENIX measurements (it can be seen directly from careful comparison of spectra given in [14] and [13]).

Values of the ratio $\langle dE_T/d\eta \rangle / \langle dN_{ch}/d\eta \rangle$ as a function of N_{part} are presented in figs. 5-8. As one can see, the position of model predictions is very regular and exactly resembles the configuration of the data in each case, the estimates are only shifted up about 10% as a whole. This indirectly proves that the earlier discussed disagreement in estimates of $dN_{ch}/d\eta|_{mid}$ and $dE_T/d\eta|_{mid}$ has its origin in the uncertainty of fitting the parameter τ (the normalization factor τ^3 cancels in the ratio). The observed 10% overestimation of the ratio can be explained, at least for more central collisions, by the observed discrepancy between the directly measured $dN_{ch}/d\eta$ and $dN_{ch}/d\eta$ expressed as the sum of the integrated charged hadron yields. If the original data points are replaced by the recalculated data, such that the denominators are sums of the integrated charged hadron yields, then much better agreement can be reached for all but peripheral collisions (see figs. 5-7).

IV. CONCLUSIONS

The single freeze-out model has been applied to estimate transverse energy and charged particle multiplicity densities for different centrality bins of RHIC measurements at $\sqrt{s_{NN}} = 130$ and 200 GeV. These two variables are independent observables, which means that they are measured independently of identified hadron spectroscopy. Since model fits were done to identified hadron data (particle yield ratios and p_T spectra) and transverse energy and charged particle

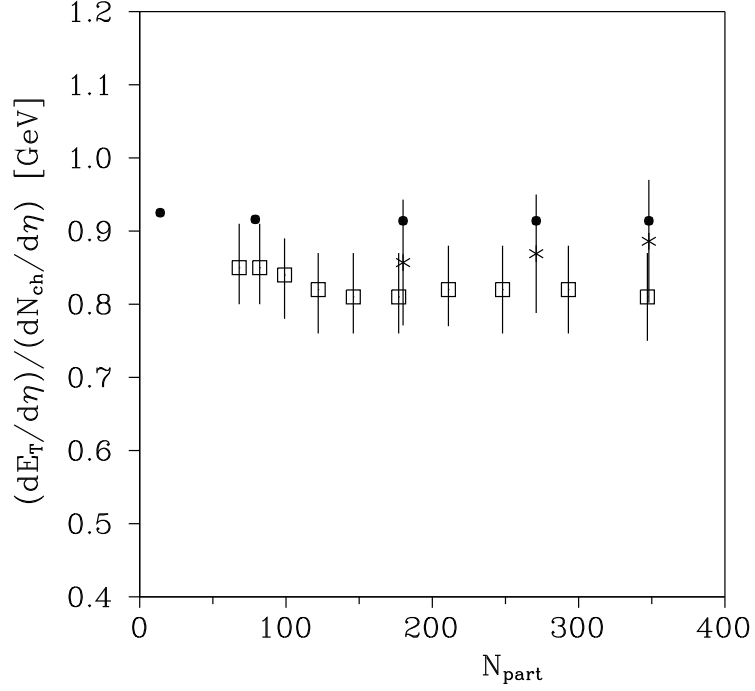


FIG. 5: $\langle dE_T/d\eta \rangle / \langle dN_{ch}/d\eta \rangle$ versus N_{part} for RHIC at $\sqrt{s_{NN}} = 130$ GeV and for the older definition of E_T , *i.e.* the total energy E_i is taken also for antibaryons in eq. (1). Dots denote model evaluations, squares are the earlier PHENIX data [8]. Crosses denote recalculated PHENIX data points, *i.e.* the sum of integrated charged hadron yields [12] have been substituted for the denominator in the ratio.

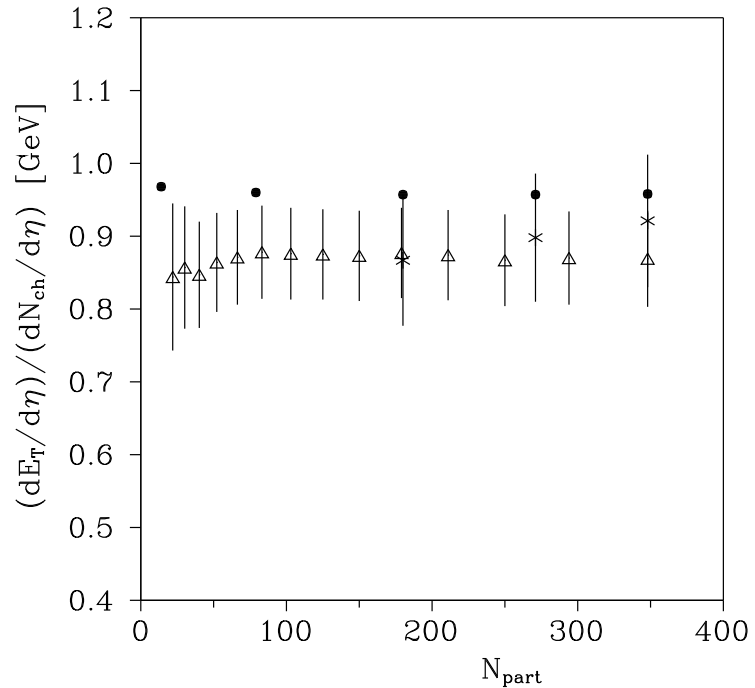


FIG. 6: $\langle dE_T/d\eta \rangle / \langle dN_{ch}/d\eta \rangle$ versus N_{part} for RHIC at $\sqrt{s_{NN}} = 130$ GeV. Dots denote model evaluations, triangles are PHENIX data [10]. Crosses denote recalculated PHENIX data points, *i.e.* the sum of integrated charged hadron yields [12] have been substituted for the denominator in the ratio.

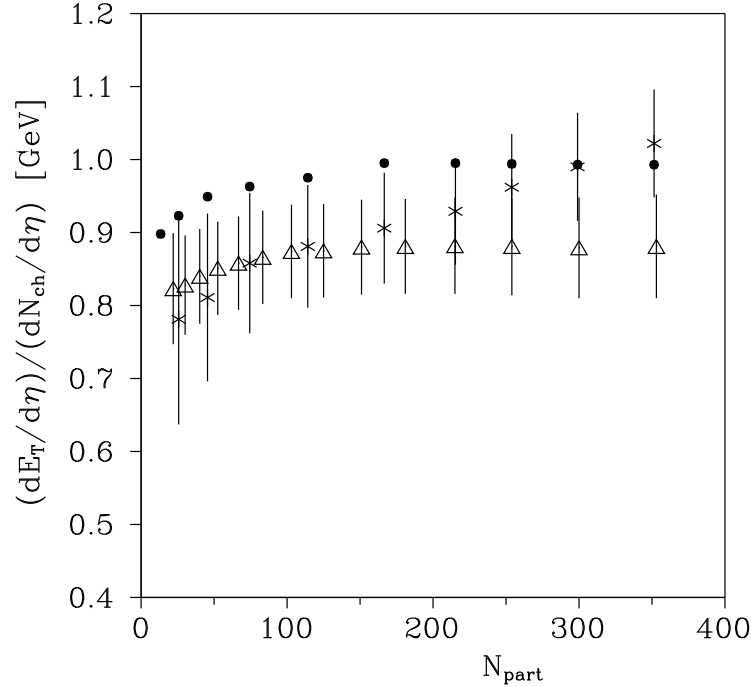


FIG. 7: $\langle dE_T/d\eta \rangle / \langle dN_{ch}/d\eta \rangle$ versus N_{part} for RHIC at $\sqrt{s_{NN}} = 200$ GeV. Dots denote model evaluations, triangles are PHENIX data [10]. Crosses denote recalculated PHENIX data points, *i.e.* the sum of integrated charged hadron yields [15] have been substituted for the denominator in the ratio.

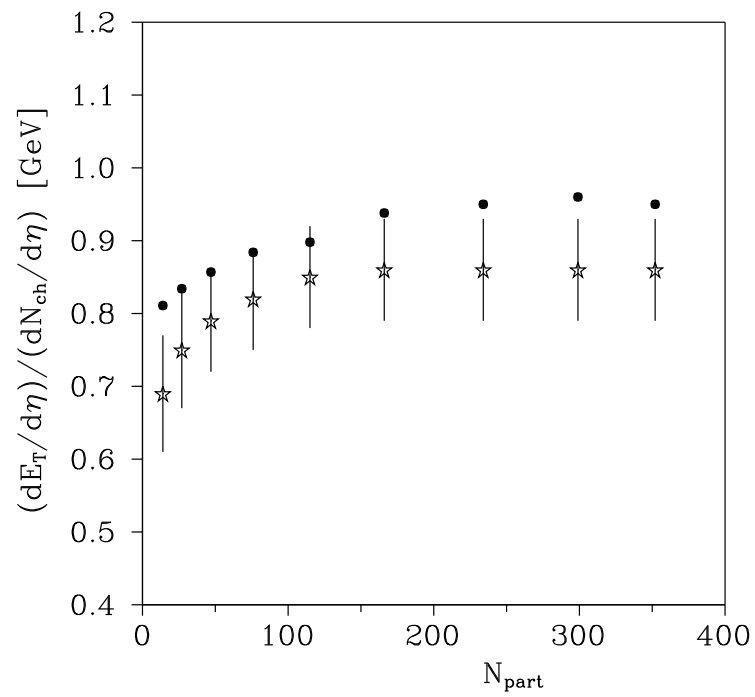


FIG. 8: $\langle dE_T/d\eta \rangle / \langle dN_{ch}/d\eta \rangle$ versus N_{part} for RHIC at $\sqrt{s_{NN}} = 200$ GeV. Dots denote model evaluations, stars are STAR data [9].

multiplicity densities are calculable in the single freeze-out model, it was very tempting to check whether their estimated values agree with the data. Generally the answer is yes, at least on the qualitative level. As it has just turned out, the main source of the quantitative disagreement is the uncertainty of the establishment of the parameter τ . The uncertainty strongly influences both densities since their theoretical equivalents contain the normalization factor τ^3 . This conclusion is confirmed by the analysis of the transverse energy per charged particle as a function of the number of participating pairs. The overestimation of at most 30% obtained for the absolute value of the transverse energy density decreases to the overall overestimation of the order of 10% for the ratio $\langle dE_T/d\eta \rangle / \langle dN_{ch}/d\eta \rangle$. On the quantitative level this means that values of only three parameters of the model are confirmed in the present analysis, namely T , μ_B and the ratio ρ_{max}/τ . Since the ratio is directly connected with the maximum transverse-flow parameter,

$$\beta_{\perp}^{max} = \frac{\rho_{max}/\tau}{\sqrt{1 + (\rho_{max}/\tau)^2}} , \quad (11)$$

this set of parameters is equivalent to T , μ_B and β_{\perp}^{max} , which are more commonly used in other statistical models describing particle production in heavy-ion collisions (e.g. the blast-wave model [17]).

To summarize, the single freeze-out version of a statistical model fairly well explains the observed centrality dependence of transverse energy and charged particle multiplicity pseudo-rapidity densities at mid-rapidity and their ratio. Since in [1] the dependence on $\sqrt{s_{NN}}$ of the above-mentioned variables was well recovered, the applicability of the single freeze-out model to the description of the soft part of the particle production in heavy-ion collisions has just been confirmed in the complete way.

Acknowledgments

This work was supported in part by the Polish Committee for Scientific Research under Contract No. KBN 2 P03B 069 25.

[1] D. Prorok, arXiv:hep-ph/0404209, submitted to Eur. Phys. J. A.
 [2] W. Florkowski, W. Broniowski and M. Michalec, Acta Phys. Polon. B **33**, 761 (2002).
 [3] W. Broniowski and W. Florkowski, Phys. Rev. Lett. **87**, 272302 (2001).
 [4] W. Broniowski and W. Florkowski, Phys. Rev. C **65**, 064905 (2002).
 [5] W. Broniowski, A. Baran and W. Florkowski, Acta Phys. Polon. B **33**, 4235 (2002).
 [6] A. Baran, W. Broniowski and W. Florkowski, Acta Phys. Polon. B **35**, 779 (2004).
 [7] K. Adcox *et al.* [PHENIX Collaboration], Phys. Rev. Lett. **86**, 3500 (2001).
 [8] K. Adcox *et al.* [PHENIX Collaboration], Phys. Rev. Lett. **87**, 052301 (2001).
 [9] J. Adams *et al.* [STAR Collaboration], Phys. Rev. C **70**, 054907 (2004).
 [10] S. S. Adler *et al.* [PHENIX Collaboration], arXiv:nucl-ex/0409015.
 [11] K. Hagiwara *et al.* [Particle Data Group Collaboration], Phys. Rev. D **66**, 010001 (2002).
 [12] K. Adcox *et al.* [PHENIX Collaboration], Phys. Rev. Lett. **88**, 242301 (2002).
 [13] T. Chujo [PHENIX Collaboration], Nucl. Phys. A **715**, 151 (2003) and
<http://alice-france.in2p3.fr/qm2002/Transparencies/20Plenary/Chujo.ppt>.
 [14] O. Barannikova and F. Wang [STAR Collaboration], Nucl. Phys. A **715**, 458 (2003).
 [15] S. S. Adler *et al.* [PHENIX Collaboration], Phys. Rev. C **69**, 034909 (2004).
 [16] A. Bazilevsky [PHENIX Collaboration], Nucl. Phys. A **715**, 486 (2003).
 [17] E. Schnedermann, J. Sollfrank and U. Heinz, Phys. Rev. C **48**, 2462 (1993).